



Short communication

## Active water management at the cathode of a planar air-breathing polymer electrolyte membrane fuel cell using an electroosmotic pump

T. Fabian<sup>a</sup>, R. O'Hayre<sup>b,\*</sup>, S. Litster<sup>a</sup>, F.B. Prinz<sup>a</sup>, J.G. Santiago<sup>a</sup><sup>a</sup> Department of Mechanical Engineering, Stanford University, Stanford, CA 94305, USA<sup>b</sup> Department of Metallurgical and Materials Engineering, Colorado School of Mines, Golden, CO 80401, USA

## ARTICLE INFO

*Article history:*

Received 12 November 2009

Received in revised form 4 December 2009

Accepted 7 December 2009

Available online 16 December 2009

*Keywords:*

Portable-power

Cathode flooding

Micro-fuel cell

Fuel cell system design

Wick

## ABSTRACT

In a typical air-breathing fuel cell design, ambient air is supplied to the cathode by natural convection and dry hydrogen is supplied to a dead-ended anode. While this design is simple and attractive for portable low-power applications, the difficulty in implementing effective and robust water management presents disadvantages. In particular, excessive flooding of the open-cathode during long-term operation can lead to a dramatic reduction of fuel cell power. To overcome this limitation, we report here on a novel air-breathing fuel cell water management design based on a hydrophilic and electrically conductive wick in conjunction with an electroosmotic (EO) pump that actively pumps water out of the wick. Transient experiments demonstrate the ability of the EO-pump to “resuscitate” the fuel cell from catastrophic flooding events, while longer term galvanostatic measurements suggest that the design can completely eliminate cathode flooding using less than 2% of fuel cell power, and lead to stable operation with higher net power performance than a control design without EO-pump. This demonstrates that active EO-pump water management, which has previously only been demonstrated in forced-convection fuel cell systems, can also be applied effectively to miniaturized (<5 W) air-breathing fuel cell systems.

© 2009 Elsevier B.V. All rights reserved.

### 1. Introduction

Air-breathing fuel cells (ABFCs) are attractive for portable power applications due to their simple construction and minimum balance of plant [1–13]. ABFCs rely on natural convection oxidant delivery, eliminating much of the cost, complexity, noise and parasitic power consumption introduced by active system design. Because ABFCs rely on natural convection to supply oxygen to their cathodes, they typically achieve much lower output power densities compared to forced-convection fuel cells.

Water management at the air-breathing cathode can present serious difficulties and cathode flooding is a frequent performance bottleneck [14–16]. Unfortunately, many of the traditional approaches to fuel cell water management are not easily applicable to planar open-cathode air-breathing fuel cell designs as there is often no direct control of the flow velocity, relative humidity, or temperature of the ambient air. Traditional techniques applicable to forced-convection fuel cells, but not to air-breathing fuel cells include positive cathode-to-anode gas pressure differential [17,18], water removal by super-stoichiometric flow [19,20] or transient purge [21,22], and water removal by the formation of a pressure gradient between a flow channel and a coolant channel

through a porous bipolar plate [23]. For detailed review see also [24,25].

Several novel water management approaches have been suggested to address the specific architecture and requirements posed by air-breathing cells. For example, Ma and Huang [26] recently introduced an air-breathing fuel cell design incorporating a piezoelectric-actuated microdiaphragm pump to improve both water removal and air delivery at the cathode. Yao et al. [27] proposed a water management design at the cathode of a miniature air-breathing direct methanol fuel cell (DMFC) based on selective hydrophilic/hydrophobic cathode patterning, variation in cathode through-hole diameter, and gravity driven droplet flow. Their architecture enables recirculation of product water but is orientation dependent. Several groups (including our own) have employed patterned hydrophilic wicks for water management in air-breathing cathodes [28–31]. Wicks can temporarily remove liquid water from the active zones of an air-breathing cathode via capillary flow. However, wicks uncoupled to an outlet cannot prevent flooding indefinitely since they have finite storage capacity and can be partially orientation sensitive.

In an effort to address these challenges, we report here on an active, scalable, low-power, orientation-independent water management design for an open air-breathing cathode based on a hydrophilic and electrically conductive wick in conjunction with an electroosmotic (EO) pump. The EO-pump actively pumps liquid water out of the water collector layer. This design builds on our

\* Corresponding author. Tel.: +1 303 273 3952; fax: +1 303 273 3795.  
E-mail address: [rohayre@mines.edu](mailto:rohayre@mines.edu) (R. O'Hayre).

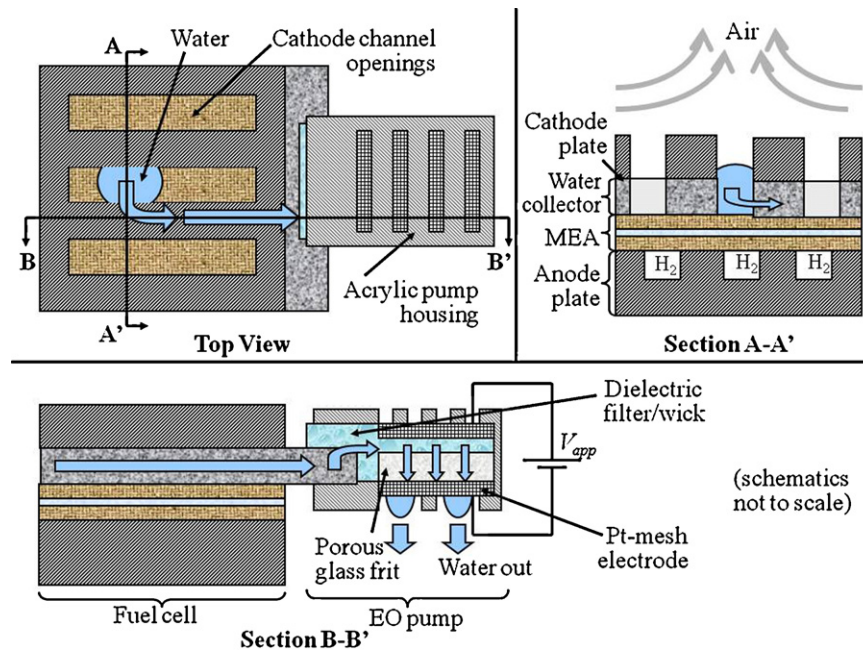


**Fig. 1.** Schematic cross-section view of an air-breathing cathode with an externally attached EO-pump hydraulically coupled to the fuel cell cathode via a porous, hydrophilic, thermally and electrically conductive wick (“water collector layer”).

previous efforts with EO-pump enabled PEM fuel cell systems [23,32] by extending their domain of application from forced-convection fuel cells into a smaller, air-breathing fuel cell. Unlike our previous designs, water removal is here accomplished by the parallel fluxes of free convection mass transport and the wick and EO-pump system. The work shows that the design concept of coupling EO-pumps with wicks can be applied to planar air-breathing fuel cell systems. We demonstrate that the EO-coupled wick system can successfully provide lateral (in-plane) water removal while not appreciably hindering vertical (normal-to-plane) air transport and water vapor transport to and from the cathode.

## 2. Materials and methods

In this section we summarize the design of the EO-pump equipped air-breathing fuel cell and the experimental measurement protocol.

### 2.1. Hydraulic design

The EO-pump-integrated ABFC design has a porous, hydrophilic, thermally and electrically conductive wick layer, we term a “water collector”. This layer is located between the gas diffusion layer and the cathode current collector plate. The water collector hydraulically links the entire area of the cathode and at the same time allows for sufficient supply of oxygen. Fig. 1 shows a schematic cross-section view of an EO-pump-equipped, air-breathing cathode with this electrically conductive water collector layer. A similar structure (without EO-pump) was described by Fabian et al. [29] in the design of a passive water management system. In the current study, the cathode water collector layer is extended beyond the active region on one side of the fuel cell in order to create a fluidic connection to the externally located  $1\text{ cm}^2$  EO-pump, as shown in the diagram. By separating the EO-pump from the basic fuel cell structure, we gain design flexibility in both structures.

Oxygen access is achieved by patterning the water collector layer with cutouts significantly larger than the pore size of the water collector while allowing for a continuous hydraulic link between any two areas of the water collector. Consequently, when

in contact with liquid water, the water collector will first saturate the volume of the small pores before blockage of the cutouts occurs. For simplicity the water collector in Figs. 1 and 2 employs a cut-out pattern identical to the openings in the cathode current collector (the cutouts in the water collector layer correspond to the openings in the cathode current collector independent cut-out patterns are also possible. In these studies, the water collector layer was fabricated from a 0.5 mm thick porous graphite plate GDM 0.5–1000 (Sigracet, SGL Technologies, St. Marys, PA). The water collector layer had a porosity of about 60%, mean pore diameter of  $38\ \mu\text{m}$ , and a water capillary rise height of 8 cm.

### 2.2. Electroosmotic pump

Electroosmotic (EO) pumps use electroosmosis to generate significant pressures and flow rates without moving parts [33,34]. Deprotonation of surface silanol groups attracts mobile counter

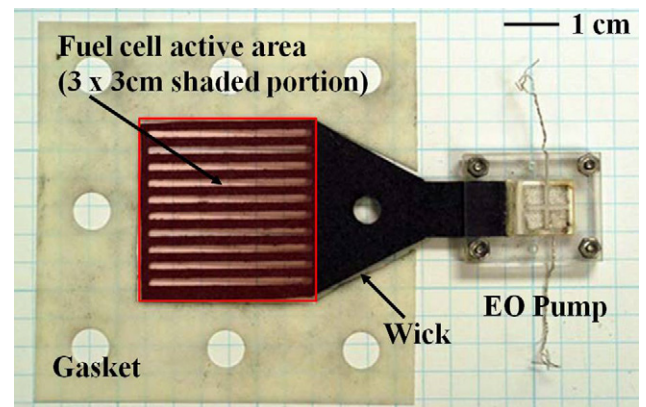


**Fig. 2.** Implementation of the wick layer with attached, external EO-pump. The wick layer area covers only the active cell area and is surrounded with a silicone gasket to minimize wick water uptake capacity and prevent gravity driven loss of water. The wick is patterned with parallel cutouts identical to the land areas of the cathode current collector.

charges in a thin (order 100 nm) diffuse layer. An applied electric field imposes a Coulombic force on this mobile charge region which causes bulk flow and pressure generation via ion-drag forces.

Fig. 1 illustrates the structure of the external EO-pump utilized in our design. An 1 mm thick and 10 mm × 10 mm porous borosilicate structure (a frit) (Robu-Glas, Germany) is fitted into an acrylic housing. The frit has a mean pore diameter of 2 μm [35]. The housing sandwiches the frit against a dielectric wick fabricated from polyvinyl alcohol (PVA) (PVA Unlimited, Warsaw, IN). This dielectric wick has a mean pore diameter of 120 μm (measured by mercury intrusion porosimetry) and provides a hydraulic coupling between the pump and the fuel cell, while reducing the electrical current between the pump and fuel cell electrode. This structure also serves as a filter for the water to reduce fouling of the pump. The other end of this dielectric wick is coupled to the conductive porous water collector. This forms a porous media path for fluid flow from the conductive water collector, to the dielectric wick, and to the frit (see Fig. 1). Once these three hydrophilic porous structures are saturated with water, water is pumped from the water collector towards the EO-pump by the slight vacuum generated at the electroosmotic pump's anode. For ease of repeatability and control of experiments, we use pure platinum meshes with 0.06 in. wire diameter (Goodfellow Cambridge Limited, UK) for the pump's anode and cathode.

### 2.3. Fuel cell hardware

The design of our air-breathing fuel cell test hardware is described in detail elsewhere [15,16,29]. Briefly, the outer dimensions of the cell are 7 cm × 7 cm × 1.5 cm, employing patterned printed circuit board (PCB)-based anode and cathode plates with parallel rib-channel geometry. The cell employed a self-humidifying, Nafion 111-based five-layer membrane electrode assembly (MEA) (BCS Fuel Cells Inc., Bryan, Texas) with 3 cm × 3 cm active area, 3 mg cm<sup>-2</sup> catalyst loading on the cathode and 0.5 mg cm<sup>-2</sup> on the anode. The water collector layer (described previously in Section 2.1), was inserted between the MEA and the PCB-based cathode current collector plate and was hydraulically connected to the EO-pump (as described in Section 2.2). Eight bolts held the complete assembly together and the torque on each bolt was 1 N m. Silicone rubber gaskets placed between the individual layers sealed the anode compartment and provided for optimal MEA compression.

### 2.4. Experimental setup

We used an experimental setup consisting of an environmental chamber (SM-3.5S, Thermotron, Holland, MI), DC load (6063B, Hewlett Packard, Palo Alto, CA), and a potentiostat (Gamry Reference 300, Warminster, PA). A detailed description of the experimental setup can be found in [16]. The air-breathing cell ran on dry hydrogen with a dead-ended anode inside of the environmental chamber. The DC load attached to the fuel cell set the current of the cell.

### 2.5. Measurement procedure

We characterized the performance of the air-breathing fuel cell with and without the electroosmotic pump by a set of polarization and galvanostatic measurements. Before each measurement, the fuel cell cathode and anode were purged with compressed air and any liquid water accumulated on or in the cell was removed. Then, the anode compartment was purged with hydrogen, the anode outlet was sealed, and the anode flow meter was checked for indications of a leak. Typical open cell voltage hydrogen flow rates were about 0.5 sccm. After the anode purge the cell was con-

nected to both the load and potentiostat and it was placed inside an environmental chamber to precisely control the ambient temperature and humidity conditions. All tests were conducted under conditions designed to exacerbate flooding [14,16,29]; namely an ambient temperature of 10 °C and an ambient relative humidity of 80% ( $T_{amb} = 10\text{ °C}$ ,  $RH_{amb} = 80\%$ ). The cell was allowed to equilibrate its temperature and membrane humidity for about 10 min before any testing.

## 3. Results and discussion

Here, we summarize our work comparing the short-term cell polarization behavior for the EO-pump-equipped air-breathing fuel cell with the EO-pump “on” and “off”. We then demonstrate the efficacy of the EO-pump and the conductive wick by removing water from an artificially flooded cathode surface.

### 3.1. Polarization measurements

Fig. 3 compares typical polarization scans of the air-breathing fuel cell for two different EO-pump voltage settings: 0 V (pump off), and 20 V (pump on). The polarization scan with the EO-pump off showed a rapid decrease of fuel cell potential above a current density of ~350 mA cm<sup>-2</sup>, consistent with the onset of severe cathode flooding. In contrast, when the pump was activated, the fuel cell cathode showed no signs of flooding and the cell supported current densities up to 600 mA cm<sup>-2</sup> above 0.4 V before the cell operation was limited by membrane dry-out (see [14–16] for a detailed discussion of the phenomenon of membrane dry-out at high current densities in this ABFC device).

### 3.2. Effect of EO-pump voltage on cathode flooding

We explored the effect of EO-pump voltage on stabilizing air-breathing fuel cell operation under severe flooding conditions. Typical data is summarized in Fig. 4. In this experiment, the EO-pump-equipped air-breathing fuel cell was operated long-term under severe galvanostatic flooding conditions  $T_{amb} = 10\text{ °C}$ ,  $RH_{amb} = 80\%$ , and  $j = 400\text{ mA cm}^{-2}$  at various pump voltages. In order to accentuate the effects of flooding, a gasket was placed around the wicking layer to minimize gravity driven water removal (see Fig. 2). Under these conditions, with the EO-pump off (zero volts), the cell voltage collapsed quickly due to flooding. The cell voltage trace was similar with an EO-pump voltage of 3 V, indicating this pump voltage was below the threshold effective voltage ( $V_{eff}$ ) for pumping sufficient water out of the wick. With an EO-pump

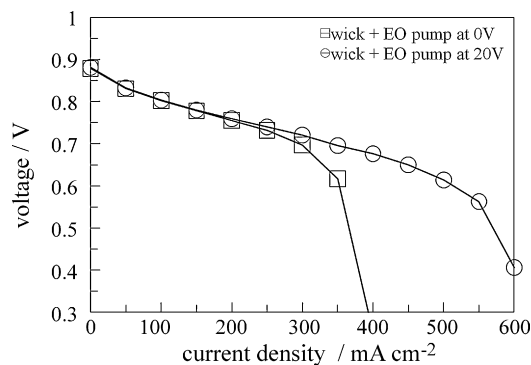
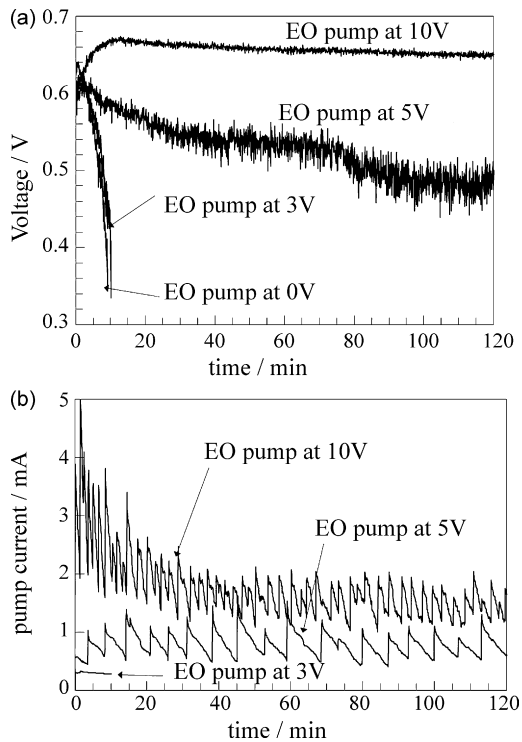
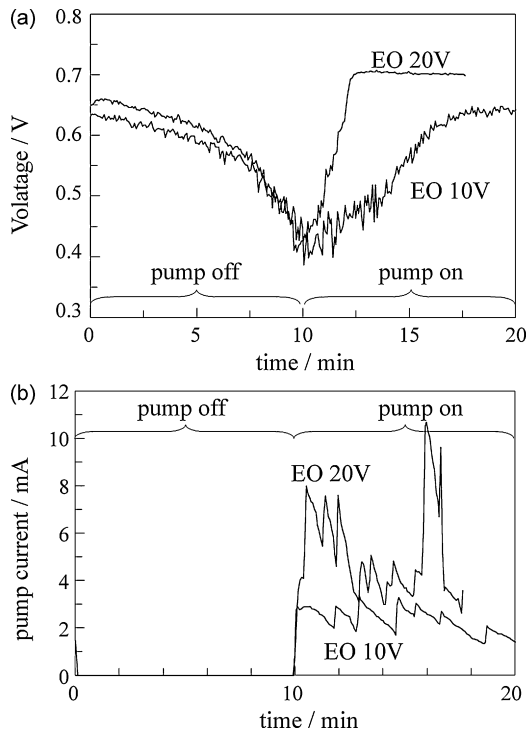


Fig. 3. Polarization scans of an EO-pump enabled air-breathing fuel cell with embedded wicking layer for EO-pump voltage settings of 0 V (pump off), and 20 V (pump on). The ambient conditions were 10 °C and 80% relative humidity and the conductive wick was 0.5 mm thick. Operation with a deactivated EO-pump leads to severe mass transport losses due to flooding. Activation of the EO-pump results in stable operation.



**Fig. 4.** Galvanostatic measurements of (a) fuel cell voltage and (b) EO-pump current in an EO-pump enabled air-breathing fuel cell with embedded wicking layer. The fuel cell was operated under flooding conditions  $T_{amb} = 10^\circ\text{C}$ ,  $RH_{amb} = 80\%$ , and  $j = 400\text{ mA cm}^{-2}$  for EO-pump voltages of 0, 3, 5 and 10V.



**Fig. 5.** Galvanostatic measurements of (a) fuel cell voltage and (b) EO-pump current in an EO-pump enabled air-breathing fuel cell with embedded wicking layer and EO-pump. The cell was operated under flooding conditions:  $T_{amb} = 10^\circ\text{C}$ ,  $RH_{amb} = 80\%$ , and  $j = 400\text{ mA cm}^{-2}$ . The EO-pump was activated at  $t = 10\text{ min}$  after flooding induced a cell voltage drop below a threshold of 0.4V. Cell recovery for EO-pump voltages of 10 and 20V applied after initial flooding is shown.

voltage of 5V, flooding was partially mitigated. An EO-pump voltage of 10V was required here to fully stabilize the cell. The pump power as well as the EO-pump power consumption relative to the generated fuel cell power can be determined from the recorded pump current, as shown in Fig. 4b. At the pump operating voltage of 10V, the EO-pump current varied between 4 and 2 mA corresponding to power consumption between 1.7 and 0.85% of the fuel cell power output. The triangular current oscillations seen in Fig. 4b are reproducible and appear to be generally characteristic of EO-pump operation in air-breathing fuel cell configurations. We hypothesize that this phenomenon reflects periodic increases in the pumping load requirement each time individual water droplets (which are nucleated in the open cut-out regions of the air-breathing cathode) grow large enough to come into hydraulic contact with the wick.

### 3.3. Effect of EO-pump voltage on transient recovery of a flooded cathode

We explored the ability of the EO-pump to “resuscitate” a flooded air-breathing fuel cell cathode. Example data is shown in Fig. 5. In this experiment, the cell was again operated in galvanostatic mode under severe flooding conditions:  $T_{amb} = 10^\circ\text{C}$ ,  $RH_{amb} = 80\%$ , and  $j = 400\text{ mA cm}^{-2}$ . Here, we first allowed the cell to flood until the voltage dropped below 0.4V, and then activated the EO-pump. We observed that the rate of cell voltage recovery increased strongly with increased applied EO-pump voltage, as expected. At an EO voltage of 10V the cell took less than 7 min to recover from a catastrophically flooded condition while at EO voltage of 20V it took less than 2.5 min to fully recover from a similarly flooded cell condition.

## 4. Conclusions

We designed and tested an air-breathing fuel cell with an integrated porous, hydrophilic, electrically conductive water collector layer coupled to an EO-pump for water removal. Steady state galvanostatic measurements suggest that the water collector layer in combination with an EO-pump can completely eliminate cathode flooding using less than 2% of fuel cell power. Short-term transient experiments show that the EO-pump can successfully resuscitate a catastrophically flooded fuel cell in a short period of time (minutes). These experiments demonstrate that EO-pump water management can be effectively applied to low-power (<5 W) miniaturized planar air-breathing fuel cell designs with only a negligible parasitic power requirement (<50 mW). This highlights the approach as a potential active water management technology for portable-power fuel cell applications.

## Acknowledgement

R. O’Hayre acknowledges support from the U.S. Army Research Office under grant #W911NF-07-1-0258 and facility support from the NSF funded renewable energy materials research science and engineering center (NSF-REMSEC) at the Colorado School of Mines.

## References

- [1] C.K. Dyer, J. Power Sources 106 (2002) 31–34.
- [2] M. Broussely, G. Archdale, J. Power Sources 136 (2) (2004) 386–394.
- [3] J.S. Wainright, R.F. Savinell, C.C. Liu, M. Litt, Electrochim. Acta 48 (2003) 2869–2877.
- [4] A. Schmitz, S. Wagner, R. Hahn, H. Uzun, C. Hebling, J. Power Sources 127 (2004) 197–205.
- [5] R. O’Hayre, D. Braithwaite, W. Herman, S.J. Lee, T. Fabian, S.W. Cha, Y. Saito, F.B. Prinz, J. Power Sources 124 (2003) 459–472.
- [6] T. Hottinen, M. Mikkola, P. Lund, J. Power Sources 129 (2004) 68–72.
- [7] T. Hottinen, I. Himanen, P. Lund, J. Power Sources 138 (2004) 205–210.

- [8] C. Ziegler, A. Schmitz, M. Tranitz, E. Fontes, J.O. Schumacher, J. Electrochem. Soc. 151 (2004) A2028–A2041.
- [9] A. Schmitz, M. Tranitz, S. Wagner, R. Hahn, C. Hebling, J. Power Sources 118 (2003) 162–171.
- [10] F. Jaouen, S. Haas, W. van der Wijngaart, A. Lundblad, G. Lindbergh, G. Stemme, J. Power Sources 144 (2005) 113–121.
- [11] S. Ha, B. Adams, R.I. Masel, J. Power Sources 128 (2004) 119–124.
- [12] J.P. Meyers, H.L. Maynard, J. Power Sources 109 (2002) 76–88.
- [13] D. Chu, R. Jiang, J. Power Sources 83 (1999) 128–133.
- [14] R. O'Hayre, T. Fabian, S. Litster, F.B. Prinz, J.G. Santiago, J. Power Sources 167 (1) (2007) 118–129.
- [15] T. Fabian, R. O'Hayre, F.B. Prinz, J.G. Santiago, J. Electrochem. Soc. 154 (2007) B910–B918.
- [16] T. Fabian, J.D. Posner, R. O'Hayre, S.W. Cha, J.K. Eaton, F.B. Prinz, J.G. Santiago, J. Power Sources 161 (2006) 168–182.
- [17] D.P. Wilkinson, H.H. Voss, K. Prater, J. Power Sources 49 (1994) 117–127.
- [18] D.M. Bernardi, M.W. Verbrugge, J. Electrochem. Soc. 139 (1992) 2477–2491.
- [19] U. Pasaogullari, C.Y. Wang, J. Electrochem. Soc. 152 (2005) A380–A390.
- [20] K. Tuber, D. Pocza, C. Hebling, J. Power Sources 124 (2003) 403–414.
- [21] H.H. Voss, D.P. Wilkinson, P.G. Pickup, M.C. Johnson, V. Basura, Electrochim. Acta 40 (1995) 321–328.
- [22] E. Antolini, R.R. Passos, E.A. Ticianelli, J. Appl. Electrochem. 32 (2002) 383–388.
- [23] J.S. Yi, J.D.L. Yang, C. King, AIChE J. 50 (2004) 2594–2603.
- [24] C.R. Buie, J.D. Posner, T. Fabian, C.A. Suk-Won, D. Kim, F.B. Prinz, J.K. Eaton, J.G. Santiago, J. Power Sources 161 (2006) 191–202.
- [25] H. Li, et al., J. Power Sources 178 (2008) 103–117.
- [26] H.K. Ma, S.H. Huang, J. Fuel Cell Sci. Technol. 6 (2009) 034501.
- [27] S.C. Yao, X. Tang, C.C. Hsieh, Y. Alyousef, M. Vladimer, G.K. Fedder, C.H. Amon, Energy 31 (2006) 636–649.
- [28] T. Fabian, R. O'Hayre, S. Litster, F.B. Prinz, J.G. Santiago, Water Management at the Cathode of a Planar Air-breathing Fuel Cell with an Electroosmotic Pump in 210th ECS Meeting, in: T. Fuller, C. Bock, S. Cleghorn, H. Gasteiger, T. Jarvi, M. Mathias, T. Murthy (Eds.), p. 949, Proton Exchange Membrane Fuel Cells 6, Cancun, Mexico (2006).
- [29] T. Fabian, R. O'Hayre, S. Litster, F.B. Prinz, J.G. Santiago, J. Power Sources, doi:10.1016/j.jpowsour.2009.12.030.
- [30] S.H. Ge, X.G. Li, I.M. Hsing, J. Electrochem. Soc. 151 (2004) B523.
- [31] S.H. Ge, X.G. Li, I.M. Hsing, Electrochim. Acta 50 (2005) 1909.
- [32] S. Litster, C.R. Buie, T. Fabian, J.K. Eaton, J.G. Santiago, J. Electrochem. Soc. 154 (2007) B1049–B1058.
- [33] S.H. Yao, J.G. Santiago, J. Colloid Interface Sci. 268 (2003) 133.
- [34] S.H. Yao, D.E. Hertzog, S.L. Zeng, J.C. Mikkelsen, J.G. Santiago, J. Colloid Interface Sci. 268 (2003) 143.
- [35] S. Litster, C.R. Buie, J.G. Santiago, Electrochim. Acta 54 (2009) 6223–6233.